aerospace

MDPI

Article

An Efficient Method for the Inverse Design of Thin-Wall Stiffened Structure Based on the Machine Learning Technique

Yongtao Lyu [1,2], Yibiao Niu [1], Tao He [3,*], Limin Shu [4], Michael Zhuravkov [5] and Shutao Zhou [6,*]

[1] Department of Engineering Mechanics, Dalian University of Technology, Dalian 116024, China; yongtaolu@dlut.edu.cn (Y.L.); nyb@mail.dlut.edu.cn (Y.N.)
[2] DUT-BSU Joint Institute, Dalian University of Technology, Dalian 116024, China
[3] Wuhan Second Ship Design and Research Institute, Wuhan 430205, China
[4] Department of Mechanical Engineering, Dalian University of Technology, Dalian 116024, China; l.shu@dlut.edu.cn
[5] Faculty of Mechanics and Mathematics, Belarusian State University, Minsk 220030, Belarus; zhuravkov@bsu.by
[6] Beijing Institute of Structure and Environment Engineering, Beijing 100076, China
* Correspondence: hetao05031213@163.com (T.H.); zhoushutao-1983@163.com (S.Z.)

Abstract: In this paper, a new method using the backpropagation (BP) neural network combined with the improved genetic algorithm (GA) is proposed for the inverse design of thin-walled reinforced structures. The BP neural network model is used to establish the mapping relationship between the input parameters (reinforcement type, rib height, rib width, skin thickness and rib number) and the output parameters (structural buckling load). A genetic algorithm is added to obtain the inversely designed result of a thin-wall stiffened structure according to the actual demand. In the end, according to the geometric parameters of inverse design, the thin-walled stiffened structure is reconstructed geometrically, and the numerical solutions of finite element calculation are compared with the target values of actual demand. The results show that the maximal inversely designed error is within 5.1%, which implies that the inverse design method of structural geometric parameters based on the machine learning and genetic algorithm is efficient and feasible.

Keywords: thin-walled stiffened structure; buckling load; back propagation neural network; inverse design

Citation: Lyu, Y.; Niu, Y.; He, T.; Shu, L.; Zhuravkov, M.; Zhou, S. An Efficient Method for the Inverse Design of Thin-Wall Stiffened Structure Based on the Machine Learning Technique. *Aerospace* **2023**, *10*, 761. https://doi.org/10.3390/aerospace10090761

Academic Editor: Zhiping Qiu

Received: 27 July 2023
Revised: 21 August 2023
Accepted: 23 August 2023
Published: 28 August 2023

1. Introduction

Due to the growing demand for space resource development, carrier rockets have gradually become a hot spot of competition in the world space field. Large thin-walled structures account for a large part of the total weight of the rocket body, which is the main skeleton of a rocket. The main failure cause of thin-walled cylindrical shells is buckling due to the loss of stability under axial pressure. To improve the stability of thin-walled structures, stiffening rib is often added to the design. The thin-walled stiffened structure is widely used in the aerospace field because of its overall light structure and strong bearing capacity [1,2]. At present, a stiffened structure is adopted in most of the key-bearing parts of carrier rockets in service [3].

Thin-wall stiffened structures are widely used in various engineering applications due to their high strength-to-weight ratio. These structures primarily endure axial loads, and their main failure mode is buckling instability [4]. Evaluating and designing the mechanical performance of thin-wall stiffened structures requires a comprehensive understanding of their behavior under different loading conditions. Traditionally, the assessment of these structures' mechanical properties has relied on theoretical calculations, numerical analysis, and experimental investigations. However, theoretical calculations often overestimate the structural performance compared to actual values for certain configurations. Conducting

experimental analysis is costly and time-consuming [5], limiting the availability of extensive results. On the other hand, finite element numerical analysis offers cost-saving advantages but can be computationally intensive for complex models, requiring several hours for each calculation. Furthermore, optimizing the design of thin-wall stiffened structures to meet specific requirements can be time-consuming [6,7].

Thin-wall stiffened structures are highly complex and characterized by a large number of design variables, such as skin thickness, rib height, width, and others. The exponential growth of these design variables poses a significant challenge in the evaluation and design of such structures. Fortunately, the rapid advancement of machine learning in the field of metamaterial design has brought new hope to address these challenges. Machine learning has demonstrated remarkable success in various fields, including metamaterial design, where it has been used to achieve efficient and accurate designs by inverse modeling. Researchers have proposed machine learning-based inverse design methods for truss lattice structures with buckling resistance [8] and nonlinear mechanical metamaterials [9]. Currently, inverse design methods can be categorized into three main approaches: indirect inverse design, semi-direct inverse design, and direct inverse design. Among these, indirect inverse design predominantly combines multi-layer perceptron (MLP) and genetic algorithms (GA). On the other hand, direct inverse design primarily employs Conditional Generative Adversarial Networks (cGAN) and Variational Autoencoders (VAE). In contrast to traditional optimization algorithms, inverse design offers higher efficiency and the ability to explore uncharted domains within the dataset. These methods leverage neural networks, such as multi-layer perceptron (MLP), and genetic algorithms (GA) to establish logical relationships between input parameters (geometric variables) and output variables (structural properties). By optimizing the predicted relationships using genetic algorithms, the inverse design process can derive the corresponding geometric parameters from desired target properties. Additionally, the researcher developed an optimization framework for lightweight metamaterials based on GAN neural networks [10]. However, there have been no reports on using inverse design methods to design the thin-walled stiffened structures.

Despite the successful application of machine learning-based inverse design methods in various fields, including optics [11], magnetic resonance devices [12], and molecular structures [13], their potential in thin-wall stiffened structure design remains unexplored. Therefore, motivated by previous research, this paper proposes a novel method combining back propagation (BP) neural networks and genetic algorithms (GA), referred to as BP-GA, for the inverse design of thin-wall stiffened structures subjected to various buckling loads. The BP-GA method uses the BP neural network to establish a latent logical relationship between geometric parameters and buckling loads [14], enabling the prediction of unknown data. Subsequently, genetic algorithms are employed to globally optimize the predicted logical relationship, resulting in the derivation of the corresponding geometric parameters from the desired structural properties. The reconstructed thin-wall stiffened structure based on the optimized geometric parameters is then subjected to finite element analysis for validation. A comparison between the initial values and the finite element calculations demonstrates the feasibility and accuracy of the machine learning-based inverse design method for thin-wall stiffened structures.

In this paper, we present the detailed methodology of the BP-GA approach for inverse design, including the data preparation, neural network architecture, genetic algorithm optimization, and reconstruction of the thin-wall stiffened structure. The effectiveness and accuracy of the proposed method are demonstrated through numerical experiments and comparisons with finite element analysis results. Finally, the potential applications and future directions of machine learning-based inverse design methods for thin-wall stiffened structures are discussed.

2. Materials and Method

2.1. Nonlinear Explicit Post-Buckling Analysis Method

With the continuous advancement of computational power, finite element-based numerical methods have made remarkable progress in accurately analyzing the behavior of thin-walled structures with reinforcements. These numerical methods consider the influences of material nonlinearity and geometric nonlinearity. For thin-walled structures, commonly used numerical analysis methods include eigenvalue buckling analysis, arc-length method, and explicit dynamics method.

In this study, the explicit dynamics method is employed as the chosen computational approach. The explicit dynamics method utilizes the central difference method to explicitly integrate the equations of motion over time. By calculating the dynamic conditions for the subsequent time increment based on the current time increment, the equations of motion can be expressed as follows:

$$\boldsymbol{M}\ddot{u} + \boldsymbol{C}\dot{u} + \boldsymbol{K}u = P \tag{1}$$

where $\boldsymbol{M}$ represents the nodal mass matrix, $\ddot{u}$ denotes the nodal acceleration, $\boldsymbol{C}$ is the damping matrix, $\boldsymbol{K}$ is the stiffness matrix, $\dot{u}$ is the nodal velocity, u is the nodal displacement and P refers to the external excitation.

At the beginning of the current time increment (at time t), the acceleration is computed using the following formula:

$$\ddot{u}_t = (\boldsymbol{M})^{-1} \cdot \left(P - \boldsymbol{C}\dot{u} - \boldsymbol{K}u\right)_t \tag{2}$$

The explicit dynamics algorithm always employs a diagonal or lumped mass matrix, simplifying the computational process. This eliminates the need for simultaneously solving the coupled equations and reduces computational costs.

The acceleration is integrated over time using the central difference method. When the velocity changes, assuming a constant acceleration, the change in velocity is added to the velocity at the midpoint of the previous time increment to determine the velocity at the midpoint of the current time increment:

$$\dot{u}_{t+\frac{\Delta t}{2}} = \dot{u}_{t-\frac{\Delta t}{2}} + \frac{\left(\Delta t_{\,t+\Delta t} + \Delta t_t\right)}{2}\ddot{u}_t \tag{3}$$

By integrating the velocity over time and adding it to the displacement at the beginning of the increment, the displacement at the end of the time increment is determined:

$$u_{t+\Delta t} = u_t + \Delta t_{t+\Delta t}\dot{u}_{t+\frac{\Delta t}{2}} \tag{4}$$

Thus, at the beginning of the increment, the acceleration satisfying the dynamic equilibrium condition is provided.

The nodal displacement can be Taylor expanded as:

$$u_{t+\Delta t} = u_t + \Delta t\dot{u}_t + \frac{\Delta t^2}{2}\ddot{u}_t + \cdots \tag{5}$$

$$u_{t-\Delta t} = u_t - \Delta t\dot{u}_t + \frac{\Delta t^2}{2}\ddot{u}_t - \cdots \tag{6}$$

From Equations (7) and (8), we can derive:

$$\dot{u}_t = \frac{1}{2\Delta t} \times \left(u_{t+\Delta t} - u_{t-\Delta t}\right) \tag{7}$$

$$\ddot{u}_t = \frac{1}{\Delta t^2} \times \left(u_{t+\Delta t} - 2u_t + u_{t-\Delta t}\right) \tag{8}$$

Substituting Equations (7) and (8) into the dynamic control Equation (1), we obtain:

$$\left(\frac{M}{\Delta t^2}+\frac{C}{2\Delta t}\right)u_{t+\Delta t}=P+\left(\frac{2M}{\Delta t^2}-K\right)u_t-\left(\frac{M}{\Delta t^2}-\frac{C}{2\Delta t}\right)u_{t-\Delta t}. \quad (9)$$

From Equation (9), it can be observed that $u_{t+\Delta t}$ is determined solely by u_t and $u_{t-\Delta t}$. Hence, the equations of motion can be directly solved without the need for iteration, and there are no convergence issues.

2.2. Datasets of the Thin-Wall Stiffened Structures

In this paper, using the finite element simulation calculation, a data set was established for the thin-walled stiffened shell structure of the four reinforcement types (orthogonally grid, anisotropic grid, angle grid, ISO grid) (Figure 1). Then, 200 samples were established for each reinforcement type, and thus a total of 800 samples were established. Among them, 600 samples were used for the training, 100 samples for the verification, and the remaining 100 samples for the testing.

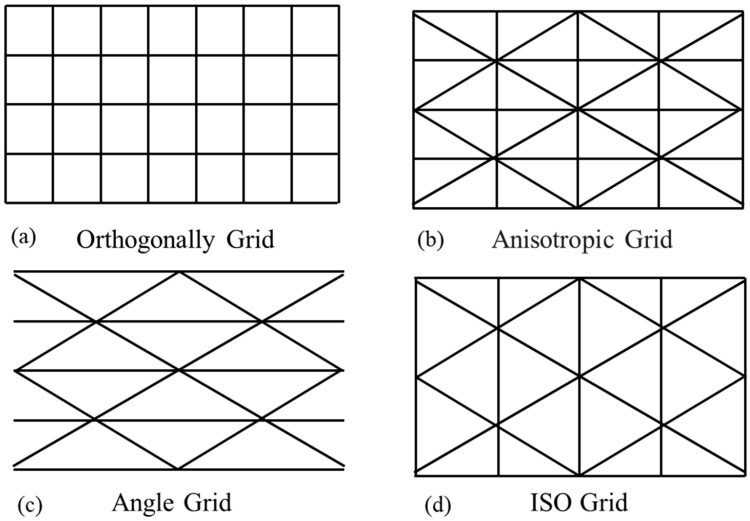

Figure 1. Four reinforcement types: (**a**) Orthogonally Grid, (**b**) Anisotropic Grid, (**c**) Angle Grid, (**d**) ISO Grid.

The structural parameters of the thin-wall stiffened structures are described in Figure 2. Figure 2b shows the cross-sectional area of the ribs. In this context, h_r signifies the rib height, w_r represents the rib width, t_s represents the skin thickness, n_1 represents the longitudinal reinforcement number, n_2 represents the ring reinforcement number, and n_3 represents the diagonal reinforcement number. The selection range of these parameters is shown in Table 1.

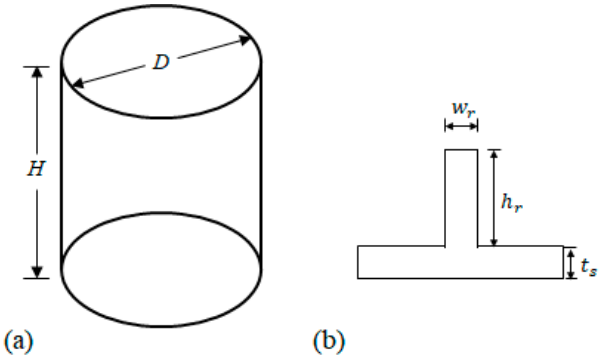

Figure 2. Sketch of the thin-walled stiffened cylinder: (**a**) geometric parameters of the thin-walled stiffened structure (**b**) geometric parameters of the rib.

Table 1. The parameters range for thin-wall stiffened structure.

Reinforcement Types	h_r (mm)	w_r (mm)	t_s (mm)	n_1	n_2	n_3
a	[2.0, 8.0]	[2.0, 4.0]	[3.0, 6.0]	[60, 80]	[10, 15]	0
b	[2.0, 8.0]	[2.0, 4.0]	[3.0, 6.0]	[60, 80]	[10, 15]	[30, 40]
c	[2.0, 8.0]	[2.0, 4.0]	[3.0, 6.0]	0	[10, 15]	[30, 40]
d	[2.0, 8.0]	[2.0, 4.0]	[3.0, 6.0]	[60, 80]	0	[30, 40]

The material of the structure is high-strength aluminum alloy. Therefore, the elastic modulus is 7.1×10^4 MPa, the material density is 2.7×10^{-6} kg/mm^3, the Poisson's ratio is 0.33, the yield stress is 503.0 MPa and the ultimate load is 540.0 MPa. The loading method was that the upper end was subjected to an axial displacement of $0.01H$, and the bottom was fully fixed. Abaqus explicit dynamics (v2020, Abaqus Inc., Providence, RI, USA) was used for the finite element calculation of the buckling load of the thin-walled stiffened structures. The element S4R was used for the thin-walled structure and the ribs, so no node binding constraint was required. The computer system used for the calculations is Windows 10, Core i5-10500, 16.0 GB memory.

2.3. BP Neural Network for Forward Prediction

Since Rumelhart et al.'s [15] pioneering work, the BP neural network model has been widely used. Its main characteristics are the forward transmission of signals and the backpropagation of errors. The BP neural network was established using in-house developed MATLAB (R2018a, Math Works Inc., Natick, MA, USA) in this paper. The complex mapping relationship between geometrical parameters (height of the rib h_r, the width of the rib w_r, the thickness of the skin t_s, etc.) and the ultimate buckling load (F_q) of aerospace thin-walled structures is discussed using the powerful nonlinear mapping capability.

The BP neural network topology with a total of n layers, including an input layer, an output layer, and n-2 hidden layers is shown in Figure 3. Its features are each layer of neurons is only fully connected with the adjacent layer of neurons, there is no connection between neurons in the same layer, and there is no feedback connection between neurons in each layer. Input variables (height of the rib h_r, width of the rib w_r, thickness of the skin t_s, etc.) and the output variable (the buckling load F_q) can be approximated by imitating the activation and transfer process from human neurons. After the prediction results are obtained using forward propagation, the errors are back-propagated layer by layer from the hidden layer to the input layer. The errors are allocated to all the elements of each layer, and the weight and threshold are adjusted by gradient, so as to obtain the optimal solution.

$$a_j^n = \sigma\left(z_j^n\right) = \sigma\left(\sum_k w_{jk}^n a_j^{n-1} + b_j^n\right) = \sigma\left(w^n a^{n-1} + b^n\right) \tag{10}$$

where $\sigma(\cdot)$ is the nonlinear activation function, w_{jk}^n is the weight of the k^{th} neuron from the $n-1$ layer to the j^{th} neuron of the n layer, b_j^n is the bias of the j^{th} neuron of the n layer, a_j^n is the value of the activation of the j^{th} neuron of the n layer, and z_j^n is the weighted sum of the output before the activation function is applied.

The activation function is very important for the BP neural network to process highly nonlinear data rather than simple linear mapping [16]. Commonly used activation functions include Sigmoid, Tanh, ReLU, etc. The activation function used in this paper is the Sigmoid function.

$$\text{Sigmoid}(x) = \frac{1}{1+e^{-x}} \tag{11}$$

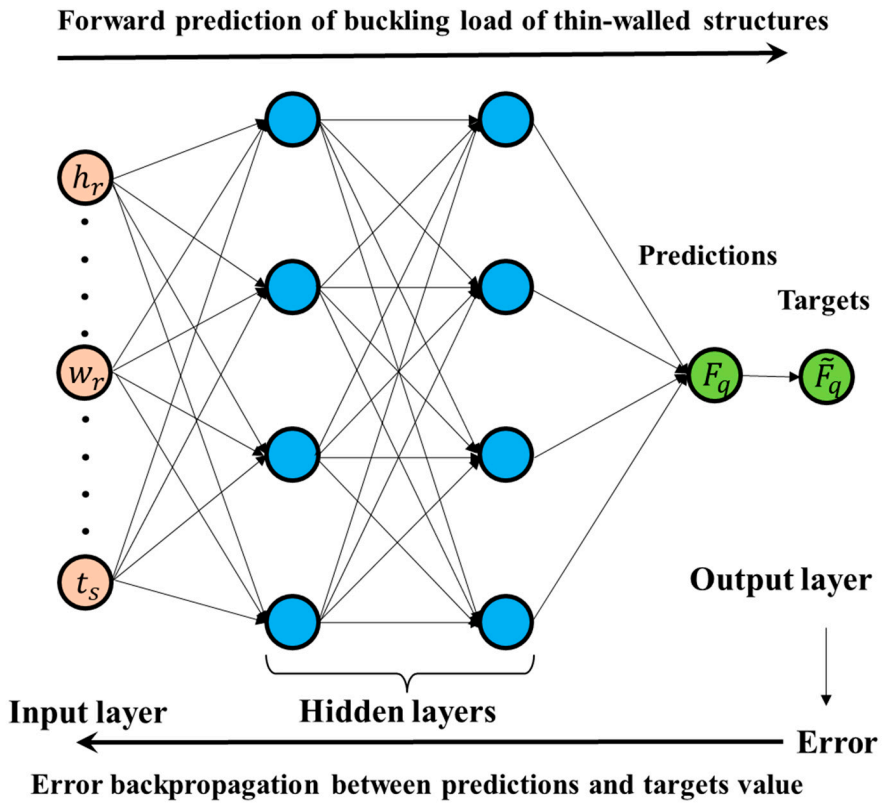

Figure 3. Structure of the BP neural network.

When the activation value of the last layer is obtained, a criterion for evaluating the prediction ability of the network is needed. Through backpropagation, the error between the network output and the expected output is minimized. The error function used in this paper is mean-square error (MSE)

$$\mathrm{MSE} = \frac{1}{n}\sum_{n}\left(\widetilde{F}_n - F_n\right)^2 \tag{12}$$

where F_n is the buckling load of the sample of the n^{th} generation, $\widetilde{F}_n$ is the predicted buckling load. When the error is less than the initial threshold, the training of the network is completed.

The coefficient of determination R^2 used in this paper is

$$R^2 = 1 - \frac{\sum_{i=1}^{n}\left(F_i - \hat{F}_i\right)^2}{\sum_{i=1}^{n}\left(F_i - \overline{F}_i\right)^2} \tag{13}$$

where F_i is the actual buckling load, $\hat{F}_i$ is the predicted buckling load, and $\overline{F}_i$ is the average buckling load.

The BP neural network structure will have a great influence on the prediction accuracy. Therefore, the parameter sensitivity of the BP neural network structure is analyzed to obtain the optimal network parameters in this paper. The influence of the prediction error is obtained by constantly changing the structure and parameters of the BP neural network. The number of hidden layers is changed in the range from 1 to 4, and the number of hidden layer neurons is selected as 6, 12, and 18.

2.4. The Structure of Improved GA

The genetic algorithm is a well-established method for solving optimization problems by simulating the process of natural selection [17]. Despite its effectiveness, traditional

GA techniques have shown vulnerabilities in terms of being trapped in local optima and exhibiting slow convergence rates. Additionally, when applied to inverse design, traditional GA can be computationally expensive and demanding. In light of these issues, this paper presents an improved genetic algorithm that introduces adaptive crossover and mutation probabilities to overcome these limitations and enhance the algorithm's performance, aiming to improve the algorithm's efficiency and global optimization capability.

The fitness function value is crucial for genetic algorithms. The fitness function in this paper is shown in Equation (14)

$$a_i = |F_i - F_i| \tag{14}$$

where a_i represents the fitness function value of the i^{th} generation, F_i represents the actual buckling load of the i^{th} generation, and F_i represents the predicted buckling load of the i^{th} generation.

Crossover, a fundamental genetic operation, involves combining genetic information from two parent individuals to generate new offspring. The crossover probability is a critical parameter governing this operation. However, traditional crossover methods may disrupt favorable parental genes. To address this challenge, an adaptive crossover probability algorithm is proposed in this study. When the fitness value of the offspring is lower than that of the parents, the crossover probability is increased (by adding an incremental probability to the initial value) to facilitate gene modification. Conversely, when the fitness value of the offspring is greater than or equal to that of the parents, the initial crossover probability is used to ensure the preservation of superior genes. Equation (15) presents the calculation formula for the incremental probability P_{c1}:

$$P_{c1} = \frac{a_{i-1} - a_i}{a_i} P_{c0} \tag{15}$$

where a_i is the value of the fitness function of the i^{th} generation and P_{c0} is the initial crossover probability.

Mutation probability is a crucial parameter in optimizing the search capability of a genetic algorithm. When a genetic algorithm approaches the vicinity of the optimal solution through the crossover operator, the local random search capability of the mutation operator can expedite convergence towards the optimum. However, traditional mutation operators may destroy parental genes when the algorithm approaches the optimal solution. Hence, during this stage, the mutation probability should be set to a smaller value. To address this issue, an adaptive mutation probability algorithm is introduced in this paper. If the fitness value of the offspring is lower than that of the parents, the mutation probability is increased (by adding an incremental probability to the initial value). Conversely, if the fitness value of the offspring is greater than or equal to that of the parents, the initial mutation probability is used. Equation (16) represents the calculation formula for the mutation probability P_{b1}:

$$P_{b1} = \frac{a_{i-1} - a_i}{a_i} P_{b0} \tag{16}$$

where a_i is the value of the fitness function of the i^{th} generation and P_{b0} is the initial mutation probability.

In this paper, the selection method used in the improved genetic algorithm was the tournament selection method. The initial values of the crossover probability and the mutation probability were both 0.1.

2.5. Inverse Design Process

The process of inverse design for thin-walled reinforced structures is shown in Figure 4. This method combines BP neural networks and genetic algorithms and encompasses several steps. Initially, a model database is established, where the input data consists of design parameters, and the output data represents the design objectives (the buckling load). Subsequently, a BP neural network is employed to construct a mapping model, facilitating

the transformation of input parameters into output data. Through the training of the BP neural network, the interconnections between neurons, including the weights and thresholds, are adjusted with utmost precision to minimize the discrepancy between the actual output data and the intended target output data.

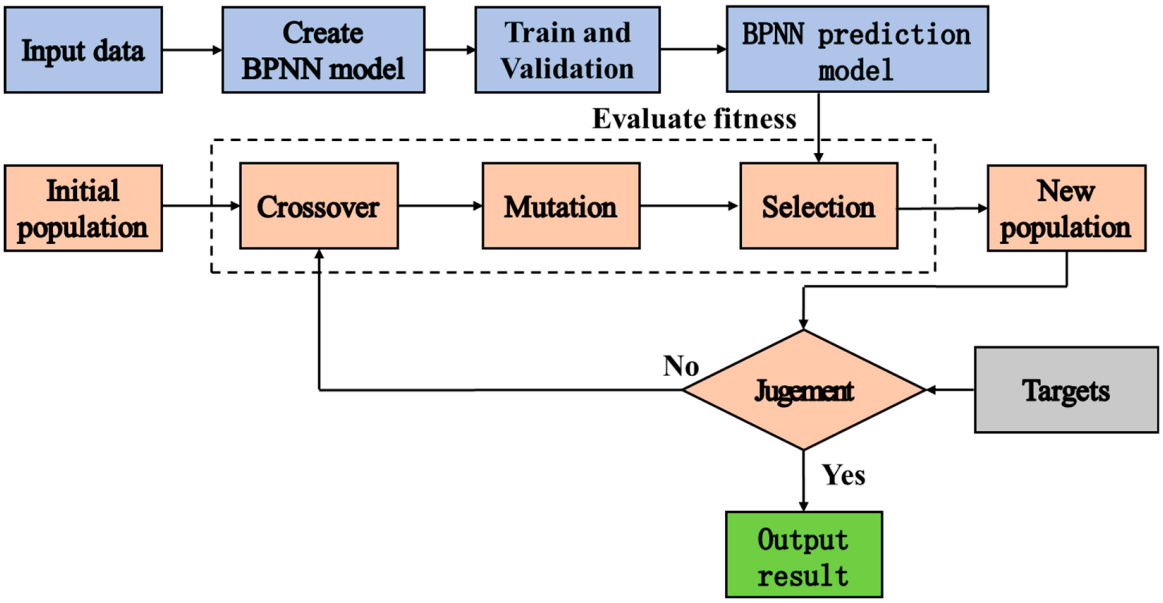

Figure 4. Flowchart for the inverse design of the structure.

Upon completion of the BP neural network training, a genetic algorithm is applied to conduct the optimization process in the inverse design. The genetic algorithm emulates natural selection and genetic mechanisms by utilizing genetic operations, including crossover and mutation, to explore the population and search for the optimal solution. Initially, an initial population is randomly generated by creating individuals with diverse combinations of design parameters. Subsequently, a selection operation is performed, evaluating the fitness function of each individual and favoring individuals with higher fitness as parents for subsequent generations. Afterward, a crossover is executed, combining the genetic information of selected parent individuals to generate offspring individuals. During the crossover operation, the probability of recombination is adjusted judiciously, aiming to preserve beneficial genetic traits while also exploring novel design spaces. Simultaneously, adaptive mutation probability is employed to introduce randomness, assisting in escaping local optima and facilitating exploration of the global optimum.

Following the creation of offspring individuals, a mutation operation is applied, involving the random modification of their genetic information. The degree of mutation is controlled by adaptive mutation probability, enabling a fine balance between diversification when offspring individuals exhibit lower fitness and preservation of superior genetic traits when fitness is higher. This methodology allows the genetic algorithm to retain advantageous genes while efficiently exploring the design space for the global optimum.

The crossover and mutation operations are iteratively performed to generate new offspring individuals and update the population. Through multiple generations of evolution and selection, individuals within the population are progressively optimized, steadily approaching the global optimum. Upon reaching the termination condition, such as reaching the maximum number of iterations or achieving the desired fitness level, the optimized combination of design parameters is obtained, serving as the outcome of the inverse design.

3. Results and Discussion

3.1. Predictive Power of the BP Neural Network

The number of hidden layers is changed in [1,4], and the number of hidden layer neurons is selected as 6, 12, and 18. The test set error after network training is shown in Figure 5. It can be found that the prediction error of using six neurons per layer in this study is small. As the number of neurons in the hidden layer increases, the prediction accuracy decreases as the number of hidden layers increases. The optimal network structure consists of two hidden layers and six neurons per layer, and the prediction error of the test set is 1.15%. Therefore, this structure is used in the subsequent prediction and inverse design.

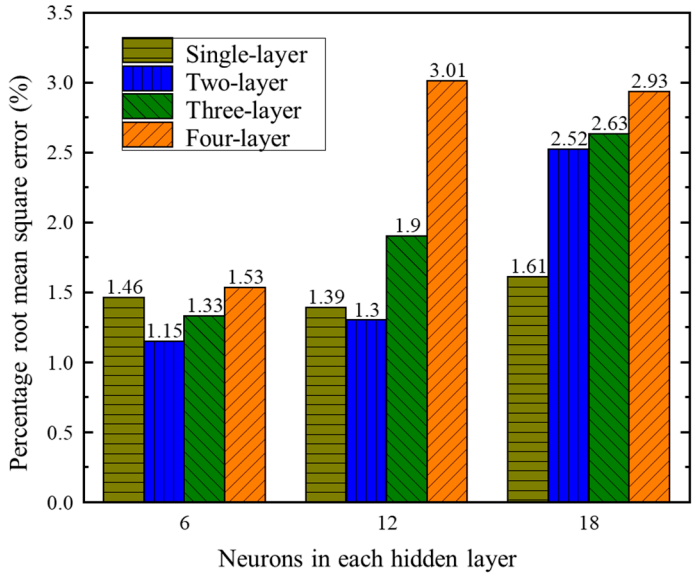

Figure 5. Sensitivity analysis of BP neural network structure parameters.

The convergence of the neural network is shown in Figure 6, and the optimal solution is obtained after the 37th epoch. The regression function is shown in Figure 7. The determination coefficient values in the training set verification set test set and all samples are 0.98, 0.99, 0.99 and 0.98, respectively, which indicates that the network has a good performance in these sets.

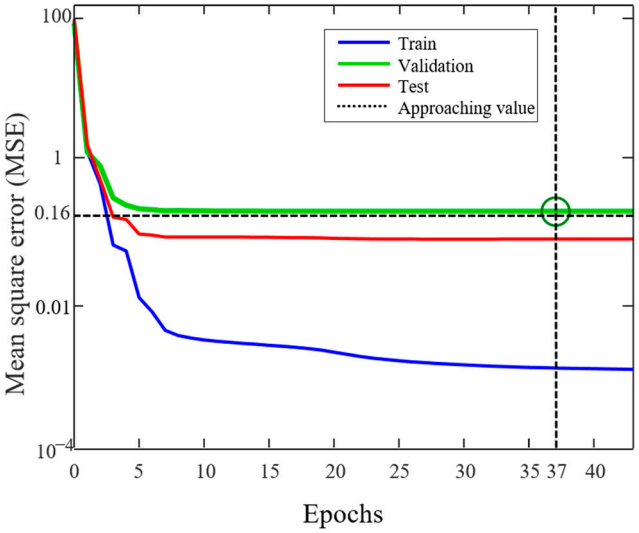

Figure 6. Convergence behavior of the BP neural network.

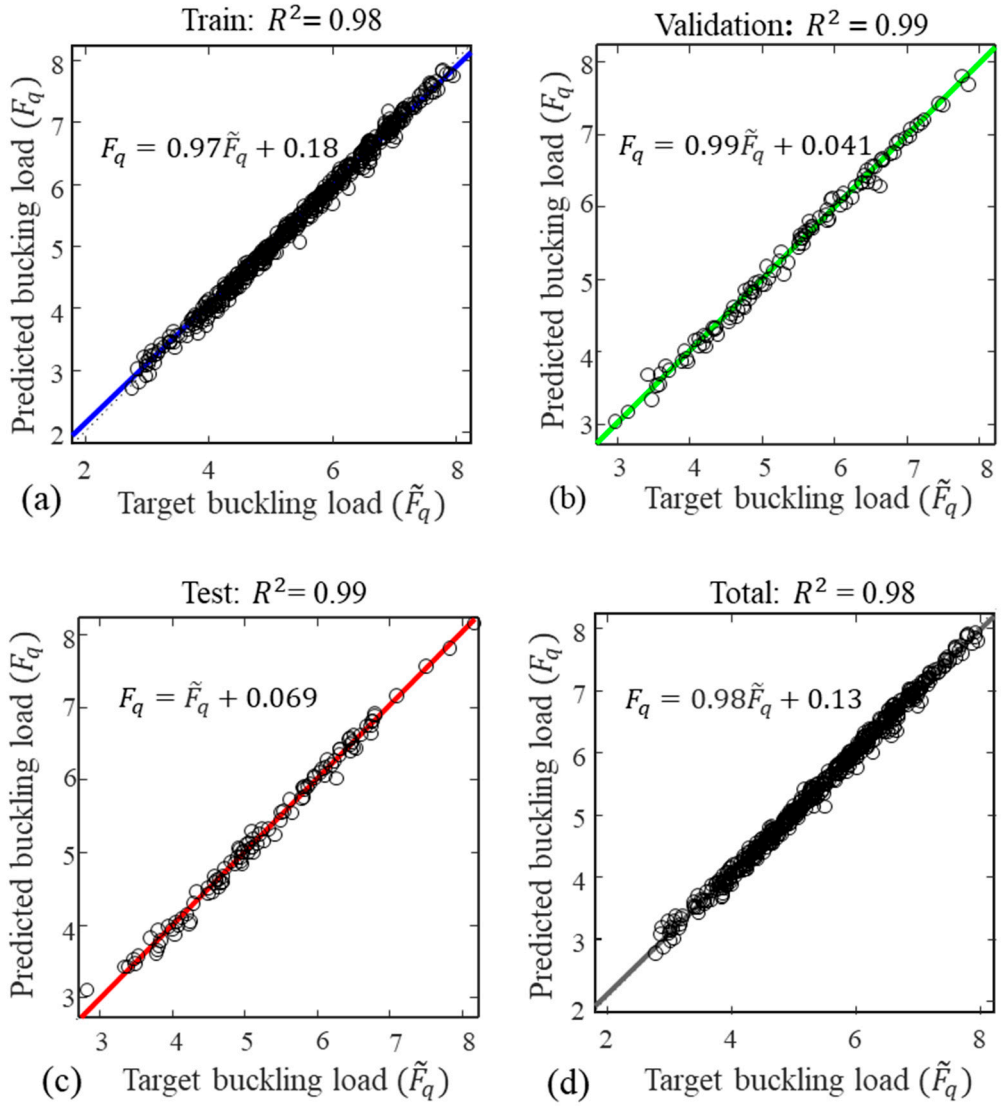

Figure 7. Regression analysis between the predicted and target buckling loads: (**a**) training data set, (**b**) validation data set, (**c**) test data set, and (**d**) overall data set.

3.2. Inverse Design of the Thin-Wall Stiffened Structure

Based on the designed BP neural network model, the improved genetic algorithm is used to inversely design the geometric parameters of thin-walled stiffened structures according to the requirements. The initial values of the crossover probability and mutation probability of the improved genetic algorithm are both set to 0.1, the number of populations is set to 700, and the maximum number of iterations is 80. The optimal structural parameters of the inverse design of the thin-walled stiffened structure with the target buckling loads in the range from 4×10^6 N to 6×10^6 N is shown in Table 2. The structural parameters obtained by the inverse design are the input for the trained BP neural network. Finally, the predicted buckling loads are compared with the target buckling loads to obtain the accuracy of the inverse design. The results in Table 2 show that the inverse design method using BP neural network and genetic algorithm can well design different reinforcement types and the obtained predictions have a good agreement with the corresponding FE results.

Table 2. Inversely designed results of the thin-walled stiffened structures.

Structure Number	Target Buckling Loads ($\times 10^6$ N)	Reinforcement Types	h_r (mm)	w_r (mm)	t_s (mm)	n_1	n_2	n_3
1	4	3	3.1	2.1	3.9	0	38	76
2	4.5	3	2.9	3.4	3.8	0	40	80
3	5	1	6.0	2.1	4.3	68	12	0
4	5.5	2	2.2	3.0	4.8	36	36	72
5	6	4	4	3.5	4.7	36	0	72

In order to further ensure the accuracy of the inverse design, the structure obtained by the inverse design is geometrically reconstructed and verified by the finite element analysis. The distributions of the obtained displacements are shown in Figure 8. The load curve of each structure is shown in Figure 9.

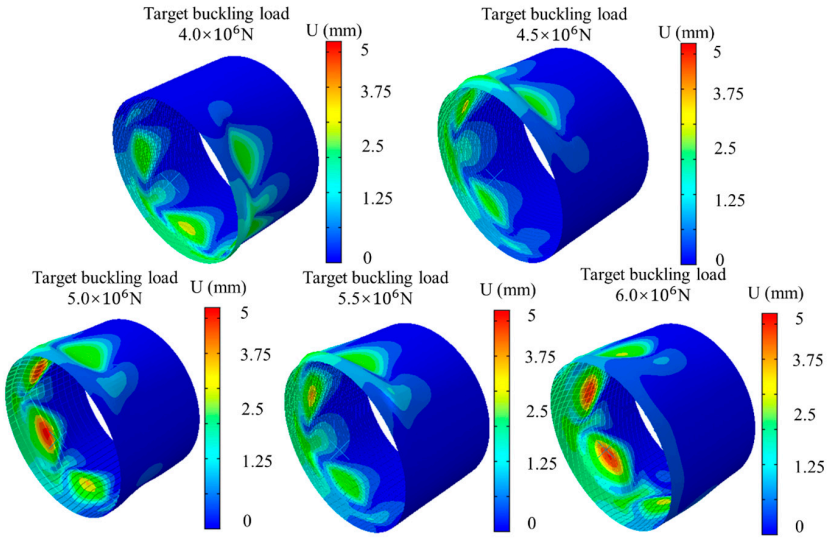

Figure 8. Distributions of the displacements for the buckled structures.

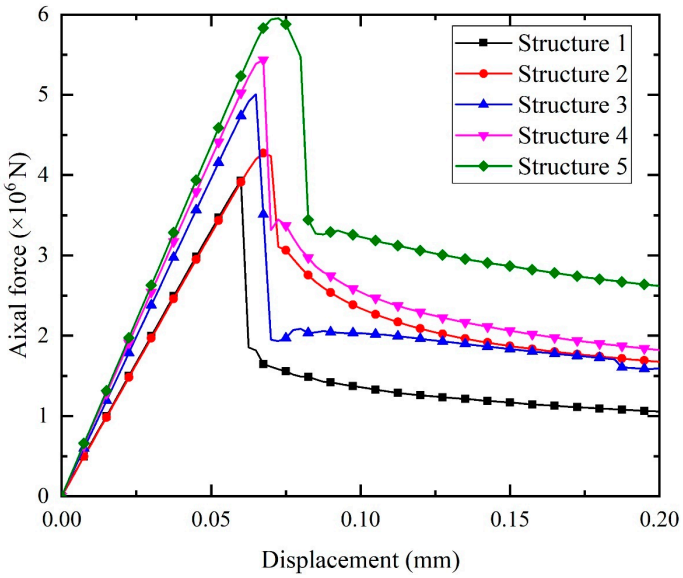

Figure 9. Load-bearing capacity of the designed structures.

The peak values in the curves shown in Figure 9 are extracted and shown in Table 3. By comparing the target buckling loads with the structural buckling loads after geometric reconstruction, it is found that the maximum error between the target buckling loads and the calculated buckling loads is only 5.1%, which proves that the inverse design method of thin-walled stiffened structures according to the required buckling load is feasible. After completing the inverse design training, it takes about one minute to perform each inverse design, which greatly saves time compared to traditional optimization design. The significant reduction in time overhead can be attributed to the streamlined nature of the proposed method. This rapid inverse design not only accelerates the entire design process, but also has the potential to accelerate the research and development cycle.

Table 3. Comparison of the inversely designed buckling loads with the target buckling loads.

Target Buckling Loads ($\times 10^6$ N)	Finite Element Calculated Buckling Loads ($\times 10^6$ N)	Relative Errors (%)
4	3.93	1.75
4.5	4.27	5.1
5	5.00	0
5.5	5.43	1.27
6	5.95	0.83

4. Conclusions

In this study, a method employing a backpropagation neural network (BP) in conjunction with genetic algorithms (GA) to accomplish the inverse design of thin-walled stiffened structures under various buckling loads is proposed. The BP neural network maps the input parameters (geometric parameters) to the output variable (buckling load) and establishes the underlying logic relationship, enabling the prediction of unknown data. The genetic algorithm performs global optimization on the predicted logic relationship, thereby deriving the corresponding geometric parameters for the desired structural properties. The reconstructed thin-walled stiffened structure is then subjected to the finite element analysis, and the results are compared against the initial values to validate the feasibility and accuracy of the machine learning-based inverse design method for thin-walled stiffened structures.

The results demonstrate that the proposed method offers a promising solution for the rapid and accurate design of thin-walled reinforced structures. By effectively addressing the complexity and challenges associated with design, this method presents numerous advantages over traditional theoretical calculations and experimental analyses, including high design efficiency, broad design domain, and enhanced accuracy.

The successful application of the machine learning and genetic algorithm-based method highlights its potential in the field of thin-walled reinforced structure design. Further research can explore and optimize this method by considering additional design variables and constraints, thereby improving design precision and reliability. Additionally, integrating machine learning with other optimization algorithms can expand its applicability to diverse fields and drive innovation and development in thin-walled structure design.

However, when preparing datasets, inverse design often takes more time than single traditional optimization methods, and the advantages of inverse design are reflected in multiple optimization designs. In terms of accuracy, we did not compare it with the experimental results. We will use experimental data to verify our results in future research.

Author Contributions: Conceptualization, Y.L. and S.Z.; methodology, Y.L., Y.N., T.H. and S.Z.; software, Y.L., Y.N. and S.Z.; formal analysis, Y.L., Y.N., T.H., L.S., M.Z. and S.Z.; investigation, Y.L., Y.N. and S.Z.; resources, T.H., L.S., M.Z. and S.Z.; data curation, Y.L., Y.N. and S.Z.; writing—original draft preparation, Y.L., Y.N., L.S. and S.Z.; writing—review and editing, Y.L., Y.N., T.H., L.S., M.Z. and S.Z.; supervision, T.H., L.S. and S.Z.; project administration, T.H., M.Z. and S.Z.; funding acquisition, T.H., M.Z. and L.S. All authors have read and agreed to the published version of the manuscript.

Funding: This study was supported by the National Natural Science Foundation of China (52241102, 12072066) and the DUT-BSU joint research grant (ICR2303), Dalian University of Technology.

Data Availability Statement: Original research data in the study are included in the article, further inquiries can be directed to the corresponding authors.

Conflicts of Interest: The authors declare no conflict of interest.

References

1. Degenhardt, R.; Kling, A.; Klein, H.; Hillger, W.; Goetting, H.C.; Zimmermann, R.; Rohwer, K.; Gleiter, A. Experiments on buckling and postbuckling of thin-walled cfrp structures using advanced measurement systems. *Int. J. Struct. Stab. Dyn.* **2007**, *7*, 337–358. [CrossRef]
2. Carrera, E.; Zappino, E.; Petrolo, M. Analysis of Thin-Walled Structures With Longitudinal and Transversal Stiffeners. *J. Appl. Mech.* **2012**, *80*, 011006. [CrossRef]
3. Huybrechts, S.; Meink, T.E. Advanced grid stiffened structures for the next generation of launch vehicles. In Proceedings of the 1997 IEEE Aerospace Conference, Snowmass, CO, USA, 13 February 1997; Volume 3, pp. 263–270.
4. Patel, S.N.; Datta, P.K.; Sheikh, A.H. Dynamic instability analysis of stiffened shell panels subjected to partial edge loading along the edges. *Int. J. Mech. Sci.* **2007**, *49*, 1309–1324. [CrossRef]
5. Lee, J.; Nguyen, H.T.; Kim, S. Buckling and post buckling of thin-walled composite columns with intermediate-stiffened open cross-section under axial compression. *Int. J. Steel Struct.* **2009**, *9*, 175–184. [CrossRef]
6. Wu, S.; Zheng, G.; Sun, G.; Liu, Q.; Li, G.; Li, Q. On design of multi-cell thin-wall structures for crashworthiness. *Int. J. Impact Eng.* **2016**, *88*, 102–117. [CrossRef]
7. Duan, S.; Tao, Y.; Han, X.; Yang, X.; Hou, S.; Hu, Z. Investigation on structure optimization of crashworthiness of fiber reinforced polymers materials. *Compos. Part B Eng.* **2014**, *60*, 471–478. [CrossRef]
8. Maurizi, M.; Gao, C.; Berto, F. Inverse design of truss lattice materials with superior buckling resistance. *NPJ Comput. Mater.* **2022**, *8*, 247. [CrossRef]
9. Deng, B.; Zareei, A.; Ding, X.; Weaver, J.C.; Rycroft, C.H.; Bertoldi, K. Inverse Design of Mechanical Metamaterials with Target Nonlinear Response via a Neural Accelerated Evolution Strategy. *Adv. Mater.* **2022**, *34*, 2206238. [CrossRef] [PubMed]
10. Challapalli, A.; Patel, D.; Li, G. Inverse machine learning framework for optimizing lightweight metamaterials. *Mater. Des.* **2021**, *208*, 109937. [CrossRef]
11. Molesky, S.; Lin, Z.; Piggott, A.Y.; Jin, W.; Vucković, J.; Rodriguez, A.W. Inverse design in nanophotonics. *Nat. Photonics* **2018**, *12*, 659–670. [CrossRef]
12. Yang, K.Y.; Skarda, J.; Cotrufo, M.; Dutt, A.; Ahn, G.H.; Sawaby, M.; Vercruysse, D.; Arbabian, A.; Fan, S.; Alù, A.; et al. Inverse-designed non-reciprocal pulse router for chip-based LiDAR. *Nat. Photonics* **2020**, *14*, 369–374. [CrossRef]
13. Gebauer, N.W.A.; Gastegger, M.; Hessmann, S.S.P.; Müller, K.; Schütt, K.T. Inverse design of 3d molecular structures with conditional generative neural networks. *Nat. Commun.* **2022**, *13*, 173. [CrossRef]
14. Caudill, M. *Neural Networks Primer, Part I*; AI Expert: Modena, Italy; Miller Freeman, Inc.: Topeka, KS, USA, 1987; Volume 2, pp. 46–52.
15. Rumelhart, D.E.; Hinton, G.E.; Williams, R.J. Learning representations by back-propagating errors. *Nature* **1986**, *323*, 533–536. [CrossRef]
16. Dubey, S.R.; Singh, S.K.; Chaudhuri, B.B. Activation functions in deep learning: A comprehensive survey and benchmark. *Neurocomputing* **2022**, *503*, 92–108. [CrossRef]
17. Li, H.; Yuan, D.; Ma, X.; Cui, D.; Cao, L. Genetic algorithm for the optimization of features and neural networks in ECG signals classification. *Sci. Rep.* **2017**, *7*, 41011. [CrossRef] [PubMed]